Mostafa Esmaeili Shayan, Gholamhassan Najafi, Giulio Lorenzini, "Optimization of a Dual Fuel Engine Based on Multi-Criteria Decision-Making Methods." *Thermal Science and Engineering Progress,* 2023,441, 102055.

Optimization of a Dual Fuel Engine Based on Multi-Criteria Decision-Making Methods

ABSTRACT

The transportation sector's need for new fuels is being addressed through the development of optimization methods, and the use of combined and alternative fuels, which will prove to be both efficient and cost-effective. This paper utilizes a multi-criteria approach, including the response surface method and Taguchi method, to evaluate several alternative fuels for a heavy-duty diesel engine. The study considers a midterm horizon to address the issue of the near future. For this purpose, the economic effects and optimization of a natural gas and diesel fuel combination were evaluated. The optimization results showed that the engine operated best at a constant speed of 1400 rpm. The results indicate that when modeling engine emissions using RSM, the effects of CO and NOx should be taken into account. When determining the optimal level of variables, it is important to increase the interval between the compression ratio and the start time of fuel injection until a specific level of emission reduction is achieved. Furthermore, Taguchi method has demonstrated that the impact of alterations in gas fuel and injection start time on the modeling of emission and performance parameters is more significant than that of other variables. The TOPSIS method was used to determine the economic, functional, and emission performance of different engine operation processes, it was found that the economic and functional criteria were aligned. However, the best solution for the environmental criterion was to focus on management.

Keywords: Response Surface Method, Taguchi Method, Heavy-Duty Diesel Engine, Optimization, TOPSIS, Environmental.

Nomenclature

Symbols		**Acronyms**	
g	Acceleration of the earth's gravity	ANFIS	Adaptive Neural Fuzzy Inference Systems
d	Arrays	ANN	Artificial Neural Networks
K	Constant coefficient	ACE	Atkinson Motorcycle
$\hat{\rho}$	Density of the fluid flow	BTDC	Before Top Dead Center
E	Entropy connection	BSFC	Brake Specific Fuel Consumption
λ	Fuel ratio	BTE	Brake Thermal Efficiency
$\dot{q}$	Heat rate	CART	Classification And Regression Tree
Y	Introduced species	CL	Closeness Index
μ	Kinematic viscosity	CNG	Compressed Natural Gas

$\hat{H}$	Local enthalpy	CFD	Computational Fluid Dynamics
$\hat{U}$	Local velocity of the fluid flow	CCM	Conventional Combustion Mode
m	Mass fraction	DFC	Dual Fuel Combustion
J	Penetration of the species	DF	Dual-Fuel
P	Probability	DORC	Dual-Ring Organic Rankine Cycle
R	Production rate	ECU	Engine Control Unit
$\hat{\tau}$	Shear stress	EGR	Exhaust Gas Recirculation
S	Source	AFR	Fuel-To-Air Ratio
δ	Stress	FIS	Fuzzy Inference System
ϑ	Stress tensor	HC	Hydrocarbon
$\hat{T}$	Temperature	IVC	Intake Valve Closing
$\hat{P}$	The pressure of the fluid flow	LHS	Latin Hypercube Sampling
ϑ	Viscosity	LCA	Life Cycle Assessment
W	Weight	LPG	Liquefied Petroleum Gas
Subscript		MCDM	Multi-Criteria Decision-Making Methods
j	Criteria	MOP	Multi-Objective Pareto Optimization
deg	Degree	NIS	Negative Ideal Points
D	Diesel	PM	Particulate Matter
g	Gaseous Fuel	PIS	Positive Ideal Points
hp	Horsepower	PER	Premixed Energy Ratios
∇	Impact of Each Parameter	CL	Proximity Distance
i,j	Local	RSM	Response Surface Meth
max	Max	SSPG	Sewage Sludge Producer Gas
min	Min	S/N	Signal-to-Noise Ratio
rpm	Revolutions per Minute	SOI	Start of Injection
t	Time	TM	Taguchi Method
u,v,w	Vectors	TMI	Thermal Management System

1. INTRODUCTION

The widespread usage of diesel engines as a propellant in industry has led to the introduction of several combustion regimes in diesel engines. The diesel/gas dual-burner engine is a type of internal combustion engine that can burn diesel and gas base fuel in varying proportions using compression ignition. In the combustion chambers of these sorts of engines, natural gas fuel is supplied indirectly and diesel base fuel is pumped directly [1]. When discussing the decrease of conventional diesel engine fuel emissions and the reduction of fuel consumption, the use of alternative fuels in diesel engines becomes significant. Natural gas is one of the alternative fuels with a basic hydrocarbon structure that are considered as clean fuels [2]. Despite the simple structure and other benefits of employing natural gas, dualizing diesel engines presents a number of obstacles [3]. Changing the combustion regime of diesel/gas dual-fuel engines impacts fuel consumption, performance metrics, and emissions [4]. On the basis of the combustion regime of diesel/gas dual-fuel engines, the parameters injection pressure, injection angle, fuel injection start time, natural gas fuel %, and compression ratio are crucial for modifying performance characteristics and emissions. With modifications to engine speed, air-fuel ratio, and injection method, these parameters can be deemed effective for modifying engine performance and emission parameters [5].

Dual-fuel engines, also known as dual-fuel internal combustion engines, are known to have lower thermal efficiency and produce higher levels of greenhouse gas emissions, including carbon monoxide and unburned hydrocarbons. Exhaust gas recirculation in certain engines can alleviate this issue to some degree[6]. In dual fuel mode, NOx emissions are expected to be reduced by an average of 30% compared to diesel mode. However, it has been observed that when using the pilot in a CNG/diesel dual-fuel engine, approximately 90% of THC methane emissions were not burned [7]. Liu and Karim began researching a multi-zone model for predicting combustion processes in dual-fuel engines in 1995. This research examines the interaction between gaseous and diesel fuels and their impact on combustion. It also describes the oxidation of gaseous fuel, operational characteristics, and greenhouse gas emissions. The results showed that the proposed model can predict the impact and pollution, which can ultimately help optimize engine performance and reduce environmental effects [8]. Luigi De Simio and Sabato Iannaccone conducted research in 2019 on the significance of alternative fuels and energy sources for technical, geopolitical, economic, and environmental reasons. They demonstrated that gaseous fuels, such as a blend of natural gas and hydrogen, can aid in mitigating greenhouse gas emissions from internal combustion engines. Their results confirmed that low-temperature combustion using gaseous fuels can enhance the combustion process of DF and decrease greenhouse gas emissions [9]. In another study, researchers used hydrogen fuel instead of natural gas to investigate the impact of exhaust gases, including carbon dioxide (CO2) emissions. Their results showed that serious issues may arise in the hydrogen diesel dual fuel engine, including abnormal combustion, poor emissions, and reduced thermal efficiency [10].

Anandavelu et al. conducted a study on the utilization of renewable biofuels in diesel engines operating in dual fuel combustion (DFC) mode. The study aimed to reduce diesel consumption and improve performance using artificial neural network and TOPSIS algorithm. The researchers also examined the emission characteristics of the engine. In this study, 1-hexanol with varying premixed energy ratios (PER) was injected into the intake port, while diesel/biodiesel was directly injected as in the conventional combustion mode (CCM). DFC mode results in a 10% increase or decrease in brake thermal efficiency (BTE) at all loads [11]. In another study, Tarafdar et al. presented a novel approach to optimize the performance and emission characteristics of a single-cylinder compression combustion engine using diesel-hydrogen dual fuel. They utilized a spherical fuzzy MARCOS MCGDM-based Type-3 fuzzy logic approach to achieve this optimization. This approach involves designing a thermal management system (TMI) with an engine control unit (ECU) to inject hydrogen into the engine manifold. The results showed a significant improvement in BTHE and a reduction in soot emissions. However, NOx emissions increased, and UHC emissions were higher at lower loads. The proposed method utilizes a fuzzy spheroid based on the MARCOS MCGDM approach [12]. In a detailed research in 2022, a valid model was used to optimize greenhouse gas emissions under compressed natural gas (CNG) operation conditions. NOx catalyst conversion efficiency under highway driving conditions was acceptable for CNG mode, but CO conversion efficiency was reported to be inadequate. The performance of the THC catalyst in gasoline was evaluated to be better due to the low reactivity of methane compared to the CNG mode after a cold start. The results showed that most of the gasoline emissions were released during cold start, while the exhaust pipe emissions increased gradually after cold start. Also, the fuel changeover time from gasoline to CNG was optimized to 48 seconds after starting the vehicle, and NOx emissions at the end of the driving cycle were reduced by 15% after optimization, but THC did not change. Optimizing THC reduction led to an increase in shift time up to 149 seconds after driving, and they reported that optimizing fuel switch timing could improve emission performance. The gap in current research is related to achieving a balanced reduction of different pollutants. There is a need to make a trade-off in optimizing the fuel switch time [13]. In another study, Ping et al. discussed the potential of utilizing waste heat energy from CNG engines by means of a dual-ring organic rankine cycle (DORC) system. This study highlights the significance of operational parameters and environmental impact in optimizing the performance of DORC systems. The bilinear interpolation algorithm is used to analyze waste heat sources and evaluate the thermodynamic, economic, and environmental performance of the DORC system. This study proposes a multi-model-based NSGA-III method for DOR [14]. In another study, Jung et al. discussed and utilized a natural gas-diesel dual fuel engine as a method for reducing greenhouse gas emissions while maintaining high thermal efficiency. This study focuses on the intake valve timing as the primary parameter that influences the air-fuel ratio, which is crucial in determining the combustion characteristics of dual-fuel engines. Researchers conducted a numerical study using 1D engine simulation to investigate the principles of dual-fuel combustion and the effects of changes in inlet valve closing during dual-fuel mode. This study showed that diesel start of injection (SOI), a key parameter in dual-fuel engines, and the intake valve closing (IVC) are independent variables. Latin hypercube sampling (LHS) was utilized to sample these variables, and a multi-objective Pareto optimization (MOP) was conducted to optimize both high thermal efficiency and low NOx emissions. Pareto-optimal solutions were obtained as a result [15]. In another study, Zhou et al. proposed a comprehensive evaluation index, 4E, which includes energy, exergy, economy, and environment, to analyze an integrated LiBr/H_2O cascade refrigeration system and Rankine organic cycle for recovering low-grade waste heat recovery. This study utilized life cycle assessment (LCA) to assess the environmental impact of the system. Additionally, a new index, Eco-indicator 16 (EI16), to combine various environmental impacts into a single quantitative score. A multi-objective optimization model has been developed. This study has provided guidance for conducting a 4E analysis of a coupled system that operates using low-grade residual heat in a cascade [16].

In 2023, a comprehensive investigation was conducted to evaluate the performance of an ignition engine utilizing sewage sludge producer gas (SSPG) as an alternative fuel. The study aimed to predict the performance of future engines with alternative fuels. A thermodynamic model was developed to determine engine performance with SSPG-methane dual-fuel blends, and response surface method (RSM) was employed to optimize engine performance and minimize emissions by adjusting combustion initiation, mixture fraction, and compression ratio. The results indicated that the optimal response was achieved with a compression ratio of 13, a 10% SSPG blend, and ignition starting at 34.09 degrees before top dead center (BTDC). The optimized responses were 35.35% ITE, 6.79 bar IMEP, 28.1% BTE, 4.6 kW BP, 5.49 bar brake mean effective pressure (BMEP), and 12.81 MJ/kWh BSEC, with CO and NO emissions of 0.645 V% and 1967 ppm, respectively. This study confirms that spark-ignition engines can effectively operate with SSPG-methane combinations, and using sewage sludge gas as a fuel source for SI engines could be a suitable option for waste valorization. The research gap was related to optimizing engine performance by adjusting input variables such as compression ratio, mixture fraction, and combustion initiation. The study has provided insights into the potential of SSPG-methane blends for efficient and low-emission engine performance, and future research could further explore this area [17]. In research, the mechanical advantages of using a dual fuel engine were investigated. In this research, Diesel-RK software is used to replace diesel with aqueous ammonia in a dual fuel diesel engine, and three different volumetric percentages of ammonia solution are being tested: 40%, 50%, and 60%. Their analysis is numerical and based on the multi-zone combustion model. The increase in ammonia solutions has caused a decrease in combustion pressure and heat release, an increase in the diameter of the burner, a delay in ignition, and a decrease in engine performance. The results showed that the brake specific fuel consumption (BSFC) variable decreased by 7.15%, 10.4%, and 15.38% for 40%, 50%, and 60% NH_4OH, respectively. Additionally, NOx emissions decreased significantly, up to 61.75%, to 60% NH_4OH. The environmental results showed that soot emissions were reduced by 43.4%, 51.04%, and 49% for 40%, 50%, and 60% NH_4OH, respectively. They suggested that aqueous ammonia can be used in dual-fuel diesel engines in order to reduce pollutants, but it must be accepted that the performance of the engine will also be reduced [18]. In a detailed research in 2023, the influence of the piston bowl geometry on the combustion performance and emissions of a dual fuel methane-diesel engine was investigated by Gulcan et al. The test variables were constant speed and five different engine loads. The results showed that the TRCC geometry also improved the emission of smoke, HC, and CO pollutants by an average of 18%, 10%, and 3%, respectively, compared to the OCC geometry. However, NO pollutant emissions were slightly higher for the TRCC geometry. They proved that the piston bowl geometry can have a significant effect on combustion performance and emissions in dual-fuel engines. A gap in their research relates to the need for more studies to fully understand the trade-offs between improved combustion and increased NO emissions with TRCC geometry [19]. In a study, Tarigonda et al. tested and discussed a dual-fuel engine that uses diesel as the ignition source and liquefied petroleum gas (LPG) as the secondary fuel. The engine was modified to accommodate LPG as a fuel source, and its parameters were optimized using Adaptive Neural Fuzzy Inference Systems (ANFIS). ANFIS combines self-learning artificial neural networks (ANN) with fuzzy inference system (FIS) reasoning. ANFIS predicted data was consistent with experimental data, with an overall correlation coefficient of 0.99415. The optimum operating conditions are an injection pressure of 194.32 bar, LPG flow rate of 1 LPM, and a BP of 1.13 with an Optimum GRG of 0.835084 [20]. In a detailed study, Goyal et al. discuss the search for alternative fuels in response to the depletion of petroleum products and the detrimental effects of emissions from combustion engines on the environment. This study aims to evaluate the performance and emission parameters of a diesel engine by using a combination of diesel and n-butanol as the test fuel, with biogas as the primary fuel. The results showed that using both pilot and primary fuel simultaneously increased BTE, hydrocarbon (HC) and CO while reducing greenhouse gas emissions. Full engine load for BTE and HC, biogas flow rate of 15 l/min for BTE, HC, and CO, and a 20% butanol composition for HC, CO and smoke [21].

Xiang et al. conducted a study on dual-fuel (DF) engines, which are a promising alternative to traditional diesel engines for reducing environmental impact and operating costs. The study aimed to optimize engine settings for marine DF engines using a computational fluid dynamics (CFD) model developed in CONVERGE software. The goal was to reduce both NOx emissions and BSFC while preventing knocking. The model was validated through pressure and greenhouse gas emission measurements in the cylinder. The study investigated engine performance settings, including pilot injection timing, equivalence ratio, and natural gas mass, under three different engine operating conditions. The results of their study showed that the optimal solution for the operating conditions of 1800 (rpm) and 1629 (rpm) can be achieved by controlling the pilot injection time, equivalence ratio, and natural gas mass within the range of -5 to -7.5 °C and -5% to gain +5. % and 0% to +20% respectively. Also, their results showed that the optimal solution for reducing NOx emissions and BSFC can be achieved by controlling the pilot injection timing, making changes to the equivalence ratio, and adjusting the mass of natural gas within specific ranges. The findings of the study support the analysis and improvement of marine DF engines during the design phase and provide guidelines for managing DF engines to reduce operating costs and environmental impact [22]. Lei Zhu et al. conducted a study on a low-speed two-stroke engine with a large bore to address the urgent need to alleviate the energy crisis and decrease greenhouse gas emissions. The study also examined the effects of fuel modification on a low-speed two-stroke marine engine equipped with EGR and an injection strategy. The findings revealed that a slight increase in indicated specific fuel consumption (ISFC) and NOx emissions occurred with an increase in the injection advance angle. This suggests that the optimal injection timing for emission and fuel consumption is 12.5 degrees CA BTDC in terms of emission and fuel consumption. An EGR rate of 10% was chosen to decrease NOx emissions and control the rate of pressure rise, which could otherwise lead to increased fuel consumption during low-temperature combustion. Fuel modification was applied to optimize fuel consumption, resulting in a 7.80% reduction in ISFC by introducing 1.29% syngas. However, this led to NOx emissions that exceeded the IMO Tier III limited emission standards. After implementing hybrid optimization, the thermal efficiency demonstrated an increase from nearly 50% (base case) to 55% with 12.5 BTDC_E10_2.25%. The study had a limitation in terms of the comparison with the base case, where NOx emissions increased but still remained below the limit value of IMO Tier III emission standards. However, ISFC reduced by 9.45% to 12.5 BTDC_E10_2.25%. In conclusion, the cooperative strategy has a high potential for improving fuel consumption and controlling emissions standards for low-speed dual-fuel marine engines [23]. Bo Yang's research has demonstrated that emissions of particulate matter, especially those composed of ultrafine particles, have a harmful effect on human health. To assess the properties of particulate emissions in a dual-fuel engine that uses diesel and natural gas, a pilot study was conducted. This paper investigates the characteristics of particle mass concentration (PM), particle number (PN), and particle size distribution (PSD) under different operating conditions of the natural gas-air mixture mode. The study investigates the impact of the timing of natural gas injection (-500° CA ATDC, -480° CA ATDC) and later (-260° CA ATDC, -240° CA ATDC) on the formation of a homogenized and classified mixture of natural gas and air-air. The fuel-to-air ratio (AFR) was maintained at a constant level throughout the test. The results indicate that the combustion process is significantly affected by the state of the natural gas-air mixture. Particulate matter (PM), especially the emission of ultrafine particles, is highly dependent on the condition of the natural gas-air mixture. Stratified mixing is an effective method for reducing the emission of smaller size PM during low load conditions. The research gap pertains to the analysis of a dual fuel engine that uses both diesel and natural gas. The study reports that over 60% of PN emissions are composed of ultrafine particles, while only slightly more than 10% do not contribute to PM emissions [24]. Proposed is the application of response surface method as a regression modeling technique to examine the performance and emission parameters of dual fuel engines [11]. Response surface method was used to predict the effect of employing hydrogen fuel as a sort of clean natural gas fuel on the emission of unburned hydrocarbons, carbon monoxide, and nitrogen oxides as the three primary pollutants in dual fuel engines. Among the characteristics of the response surface method are presenting the regression relationship of emission owing to the change of two factors, hydrogen fuel precentage and engine load, and assessing the mutual changes of independent variables [25]. Experimental design, regression modeling, and single-objective optimization are some of the hallmarks of response surface method [26]. To this end, a study was done to determine the impact of biodiesel fuel made from kitchen waste oils on the emission and performance parameters of a dual fuel biodiesel engine [27]. Xilei Sun et al. conducted an experimental investigation to analyze the impact of injection timing, injection pressure, and exhaust gas recirculation (EGR) rate on the combustion, thermodynamic, and emission characteristics of the Atkinson motorcycle (ACE). The study aimed to improve the overall performance of the ACE by utilizing a machine learning method for multi-objective optimization. The researchers conducted an engine bench test to collect relevant characteristic parameters, which were utilized as the data basis for model building. Three tree-based machine learning models, namely Classification and Regression Tree (CART), Random Forest, and Adaptive Boosting (AdaBoost), were developed for the ACE. Random Forest was built using a parallel method, while AdaBoost was built using a serial method. Both models used CART as the base learner. The AdaBoost model and NSGA II algorithm were utilized to perform multi-objective optimization of the combustion, thermodynamic, and emission characteristics of the ACE. The results indicated that the three tree-based models exhibited high prediction performance and generalization ability. Among them, AdaBoost demonstrated the best performance, followed by RF and CART. The serial method (AdaBoost) was found to be superior to the parallel method for the dataset. The study revealed that the second non-dominated solution, which optimized brake specific fuel consumption (BSFC), and the fourth (optimal PN) had a significant impact on reducing emissions compared to the experimental data of the main engine. Specifically, they reduced CO, BSFC, NOx, and PN by 31.9%, 2.3%, 39.1%, and 61.6%, 32.3%, 2.2%, 40.0%, and 62.6%, respectively [28]. The experimental design of response surface method permits the evaluation of the combination of many qualitative independent variables as different treatments in the modeling of performance parameters and pollutant emissions [29]. Fuel injection technique is one of the qualitative independent factors. Response surface method was used to describe and optimize the research of combustion, performance, and emission characteristics for three injection strategies: multi-section injection, continuous injection, and combined injection-continuous injection [30].

The Taguchi method (TM) is another statistical technique used to estimate the output characteristics of internal combustion engines. This strategy addresses the limits and weaknesses of response surface method [31]. The Taguchi method involves designing an orthogonal test matrix and determining the optimal levels of independent variables. The optimal timing and volumetric flow rate for hydrogen injection were investigated for various operating conditions of a diesel/hydrogen dual-fuel engine [32] based on the characteristics of Taguchi's statistical scheme. Using a combination of Taguchi modeling and multi-objective optimization, the effects of engine load, injection pressure, and EGR were investigated. Using Taguchi modeling [33], the problem of specifying the levels of variables and the effect of isolating pollution emission models was resolved. Modeling and optimization techniques can be regarded effective for establishing the ideal engine operation answer category [34]. The decision to select the ideal parameters under various engine operating situations has been debated as a result of the various ways to determining the optimal engine operation [35]. Multi-criteria decision-making methods have made it possible to determine the optimal decision based on engine functional approaches [36]. Choosing the optimal answer category is the outcome of optimization and analysis of multiple engine methodologies, including the TOPSIS method [37,38].

This study aims to simulate, model, and optimize a sample diesel/gas dual fuel engine. To achieve this goal, we simulated the combustion process of a dual-burning diesel/gas engine using computational fluid dynamics and analyzed the pollution effects of its operational parameters using modeling techniques. This research is innovative in its utilization of the Taguchi approach to rank variables and report their average influence on the economic performance of a dual fuel engine.

2. MATERIALS AND METHODS

Due to the extensive scope of numerical analysis and its connection with modeling and optimization, the importance of researching modeling approaches was emphasized in this investigation. However, it is required to provide a brief description of the appropriate procedure for conducting combustion simulation studies using computational fluid dynamics. The technical specifications of the engine, the pre-processing of the solution field, the governing equations, the processing of the solution field, and the validation of the results, including combustion simulation procedures, are all addressed using the computational fluid dynamics approach. The D2676-LE475 heavy-duty diesel engine is commonly used for urban transportation and marine applications. Table 1 displays the parameters for the D2676-LE475 diesel engine in accordance with DIN ISO 3046-1.

Table 1. Technical specifications of the dual fuel diesel engine (D2676-LE475) [17]

Technical Features	Value	Technical Features	Value
Displacement (l)	12.42	Speed (rpm)	1000-1600
Nominal Rating (kW (hp))	221 (301)	Lowest specific fuel consumption (g/kWh)	206
Rated Speed (rpm)	1800	Classifiable	Yes
Maximum Torque (N.m)	1731	Exhaust gas after treatment	Yes

2.1. Computational Fluid Dynamics Simulation

The initial and boundary conditions for the solution field are defined during the processing stage of the solution process. Figure 1 illustrates the scope of the solution domain, while Table 2 presents the initial and boundary conditions for the solution.

Table 2. Boundary conditions for the solution field

Characteristic	Condition	Characteristic	Condition
Time to Start Spraying	16 deg BTDC	Cylinder Head	Wall- Temperature 590 K
Air Valve Closing	120 deg BTDC	Piston	Mesh Movement-Temperature 600 K
Opening the Smoke Valve	116 deg ATDC	Cylinder Head Wall	Wall-Temperature 580K(Heat Flux=0)
Initial Pressure	1/2 time	Axis of the Figure	Symmetry
Initial Temperature	360 K	Fuel Inlet and Outlet	Periodic Inlet/Outlet

The ignition issue of the diesel/gas dual-fuel engine was resolved by utilizing AVL FIRE software. The majority of traditional software used to investigate fluid behavior approaches the subject from a Eulerian-Lagrangian perspective. The method employed for the software solution is volume control. The ESE Diesel module handled the generation of the geometry and grid for the solution domain. The average size of the original grid was set to be 22 mm. The use of a moving mesh was also considered to accommodate the reciprocating motion of the piston within the solution field. Due to the unique conditions of gas and diesel combustion, the Fire-Comkin coupler was utilized to describe the combustion process. N-heptane (n-C7H16) was selected as the fuel for spraying. Natural gas was used as the initial condition in the solution field and was mixed with air. The study utilized GRI-Mech 3.0, which integrates chemical kinetics and n-heptane combustion. It includes 76 species and utilizes 464 reaction mechanisms [18]. The injection of liquid fuel starts the self-ignition process. Figure 1 shows the piston sector and how the solution field is gridded.

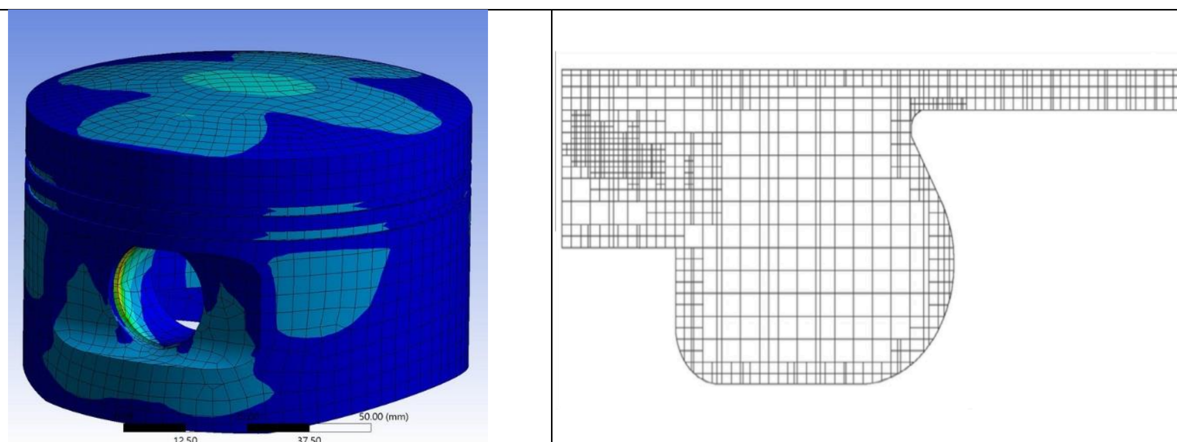

a b

Figure 1. Piston sector and field grid

Combustion modeling for compression ignition engines involves several equations, including the survival equation, momentum equation, energy equation, species transfer equation, turbulence equation, combustion model, emission equations, air-fuel ratio equation, and evaporation equations for sprayed particles. Methods of numerical discretization are used to solve the equations. The relationships used to describe fluid flow behavior in the solution field will be solved in the Cartesian coordinate plane. If the velocity of the fluid flow at the center of the control volume is defined as a vector $\vec{V} = (u, v, w)$, the survival relation is as follows.

$$-\frac{\partial \rho}{\partial t} = \frac{\partial(\rho u)}{\partial x} + \frac{\partial(\rho v)}{\partial y} + \frac{\partial(\rho w)}{\partial z} \tag{1}$$

The Navier-Stokes equation describes how changes in fluid flow speed and pressure are interdependent across different dimensions.

$$\begin{aligned}\hat{\rho}\frac{D\hat{U}_{i}}{Dt} &= \hat{\rho}\frac{\partial \hat{U}_i}{\partial t} + \hat{\rho}\hat{U}_{i}\frac{\partial \hat{U}_{i}}{\partial x_j} = \hat{\rho} g_i + \frac{\partial \widehat{\sigma_{ij}}}{\partial x_j} \\ &= \hat{\rho} g_i - \frac{\partial \hat{P}}{\partial x_i} + \frac{\partial}{\partial x_j}\left[\mu\left(\frac{\partial \vartheta_i}{\partial x_j} + \frac{\partial \vartheta_j}{\partial x_i} - \frac{2}{3}\frac{\partial \vartheta_K}{\partial x_K}\delta_{ij}\right)\right]\end{aligned} \tag{2}$$

Where, $\hat{U}_i$ is the local velocity of the fluid flow, $\hat{\rho}$ the density of the fluid flow, g_i the acceleration of the earth's gravity, $\hat{P}$ the pressure of the fluid flow, μ the kinematic viscosity, ϑ_j and ϑ_i the stress tensor between the fluid flow lines and δ_{ij} the stress resulting from the interaction of the fluid flow with the wall of the solution field Is. The enthalpy equation represents the heat output from combustion, heat transfer near the walls, and the rate of heat release, all of which affect the performance parameters of the power indicator. The energy equation can be represented by the following continuous polynomial.

$$\hat{\rho}\frac{d\hat{H}}{dt} = \hat{\rho}\left(\frac{\partial \hat{H}}{\partial t} + \hat{U}_{j}\frac{\partial \hat{H}}{\partial x_j}\right) = \hat{\rho}\dot{q}_g + \frac{\partial \hat{P}}{\partial t} + \frac{\partial}{\partial x_i}\left(\widehat{\tau_{ij}}\hat{U}_{j}\right) + \frac{\partial}{\partial x_i}\left(\lambda\frac{\partial \hat{T}}{\partial x_j}\right) \tag{3}$$

Where, $\hat{H}$ is the local enthalpy of the fluid flow, $\dot{q}_g$ is the exchange heat rate in the natural gas mixture, $\hat{\tau}_{ij}$ is the shear stress between the fluid flow lines, λ is the fuel ratio and $\hat{T}$ is the temperature of the fluid flow [19]. The transfer of species involves the precise measurement of all species, as well as the methods of mixing, penetration, and evaporation of two fluid phases. In order to describe the reaction kinetics of dual-fuel diesel engines, the behavior of each species involved in the reaction must be estimated. This is done by analyzing the species transfer relationship at each step of the reaction [20]:

$$\frac{\partial}{\partial t}(\rho Y_i) + \nabla(\rho\vec{v}Y_i) = -\nabla\vec{J_i} + R_i + S_i \tag{4}$$

Where, Y_i represents the introduced species, ϑ is the viscosity of the fluid flow, J_i determines the penetration of the species, R_i is the production rate of the species after the reaction and S_i is the source of the species created in the previous reaction and enters the new equation. Determining the percentage of natural gas in the fuel mixture is a crucial parameter in determining the combustion quality of dual-fuel engines that use both diesel and gas. According to the position of the gas valve during half-load operation, the percentage of natural gas fuel input can be determined using Equation 5.

$$CNG(\%) = \frac{\mathrm{m}_g \,.\, LHV_g}{\mathrm{m}_D \,.\, LHV_D + \mathrm{m}_g \,.\, LHV_g} \tag{5}$$

where m_{g} and $\mathrm{m_D}$ are the mass fraction of natural gas fuel and injection fuel, respectively.

2. 2. VARIABLES AND MODELING

Several factors influence the combustion process in dual-fuel engines that use diesel and gas. Among these factors are engine speed, the proportion of diesel fuel and gas mixture, diesel fuel injection pressure and timing, diesel fuel injection angle, compression ratio, and other engine parameters. The study evaluated several input variables, including the percentage of diesel fuel and gas mixture, the start time of diesel fuel injection, the angle of diesel fuel injection, and the compression ratio of the engine. It is important to note that this study utilized a combustion simulation approach and numerical computational fluid dynamics techniques. The results were validated and used as inputs or outputs for the model. Due to the absence of experimental design in the numerical simulation, it was not possible to match all input and output parameters with the modeling unit's methodologies. Consequently, a portion of the inputs and outputs were evaluated each time using a new modeling technique. Input and output variables were studied using three methods: response level method, the Taguchi method, and the multi-criteria decision-making method. These methods were chosen based on knowledge gained during the relevant course unit regarding the capabilities and limitations of various modeling methods.

2.2.1 Response Surface Method (RSM).

By applying the response surface method approach to investigate and match the input and output variables, we established the optimal conditions for studying the emission characteristics of the diesel/gas dual-fuel engine. Three variables were examined as input factors. Therefore, the Box-Behnken approach was chosen for parameter analysis and modeling. In this method, the range of changes for input parameters in the model (established ceiling and floor levels for input variables) is divided into three parts, and the arithmetic mean of the change range for each input is calculated. The test matrix for modeling using response surface method is presented in Table 3.

Table 3. Modeling a Test Matrix in Response Surface Method.

Row	Variable	Level (change interval)	Unit
1	Diesel Fuel Injection Start Time	18 to 35	deg-BTDC
2	Fuel Injection Angle	140 to 160	deg
3	Compression Ratio	16 to 18	_
	Response		
	Carbon Oxides (CO)	-	ppm
	Nitrogen Oxides (NOx)	-	ppm

In the Taguchi method, three pre-processing stages are performed to generate an appropriate Taguchi modeling response based on the type and number of inputs. The number of elements and levels must be determined before constructing the Taguchi model. Taguchi's method determines the number of tests required for his study. The second phase determines the status of the output variable based on its data type. This stage also determines the graphs required to assess variable behavior. A test matrix can help determine the number of factors and their corresponding levels. The test matrix of each research study determines the levels and changes of input variables. It is important to note that a poorly designed test for experiments can lead to issues in the test matrix design and Taguchi method, which can prevent the statistical plan from being orthogonal.

Table 4. The Taguchi Method Variables.

Variable	Unit	Level 1	Level 2	Level 3	Level 4
CNG	%	65	52	22	-
SOI	deg-BTDC	15	18	30	35
Spray Angle	deg	140	150	160	-
CR	-	15.5	16	16.5	17.5
Response					
Fuel Consumption and Efficiency	BSFC (gr/kWh)				
Functional Outputs	T (N.m)				
Emissions	CO (ppm)		NOx (ppm)		EGT (K)

2.2.2 Multi-Criteria Decision-Making Method (TOPSIS)

Multi-criteria decision-making methods (MCDM) used in engine parameter studies enable the optimization of system performance. These technologies give combustion engine control systems decision-making power. Fluid simulation of the combustion process in a dual-fuel diesel/gas engine produces a wide range of outputs. In order to utilize the multi-criteria decision-making process, it is necessary to categorize the options or alternatives being considered. On this basis, three approaches to separating outputs were studied: economic, functional, and environmental. Additionally, we examined the variations of each category of input variables as a determining factor. The economic outputs of the engine were evaluated using specific braking fuel consumption, indicative specific braking fuel consumption, and braking thermal efficiency metrics. The economic decision-making strategy is to minimize fuel consumption and maximize thermal efficiency during braking. Performance characteristics, torque parameters, indicator power, average indicator average pressure, and average brake average pressure were evaluated. The maximum value for all output parameters was found using the multi-criteria decision-making technique to evaluate the performance of the investigated engine. As a result of the environmental approach, the parameters for emissions of pollution and exhaust gas temperature were determined. In the environmental approach, decision-making is based on minimizing pollution and reducing the heat generated by exhaust gas emissions. Figure 2 illustrates the process of categorizing output variables.

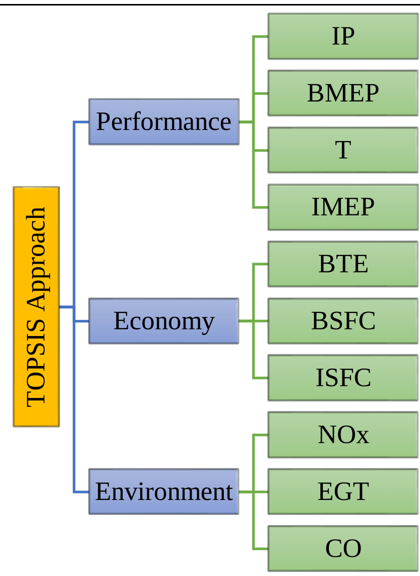

Figure 2. TOPSIS Method Classification of variables.

The decision matrix is designed to express options and criteria mathematically. In reality, the decision matrix has dimensions of m × n, where m represents alternatives and n represents criteria. In Equation 7, the process of constructing the choice matrix is illustrated.

$$D = \begin{bmatrix} d_{11} & \cdots & d_{1*n} \\ \vdots & \ddots & \vdots \\ d_{m*1} & \cdots & d_{m*n} \end{bmatrix}_{m*n} \tag{7}$$

Using the following relationship, the change range of the options can be constrained to a specified range. The normalizing matrix is depicted by Equation 8.

$$n_{ij} = \frac{d_{ij}}{\sqrt{\sum_{i=1}^{m} d_{ij}^2}} \qquad 0 \leq n_{ij} \leq 1 \tag{8}$$

In relation 8, d_{ij} is the arrays of matrix D. After creating n_{ij}j values, equation 9 describes how to form the normalization matrix.

$$N = \begin{bmatrix} n_{11} & \cdots & n_{1*n} \\ \vdots & \ddots & \vdots \\ n_{m*1} & \cdots & n_{m*n} \end{bmatrix}_{m*n} \tag{9}$$

Normal matrix weighting involves assessing normalized options based on their importance. This weighting can be achieved through either expert opinion or Shannon's entropy technique. The Shannon entropy weighting approach utilizes the Shannon entropy normal distribution method, which is commonly used in information science and data mining, to analyze and statistically evaluate the uncertainty of data. This method was presented to minimize the non-uniformity of weightings based on expert opinions. By doing so, it reduces the dependence on expert opinions and establishes the necessary uniformity for the production of the lambda matrix. This method defines uncertainty for each criterion using Equation 10.

$$E_j = -k \sum P_{ij} \ln(P_{ij}) \tag{10}$$

In equation 10, K is a constant coefficient for normalization, and P_{ij} is the probability of the *i* option occurring in the *j* criterion. Equation 11 is provided for calculating the K coefficient, while Equation 12 is proposed for calculating the P matrix.

$$K = \frac{1}{\ln(m)} \tag{11}$$

$$P_{ij} = \frac{d_{ij}}{\sum_{i=1}^{n} d_{ij}} \qquad 0 \leq P_{ij} \leq 1 \tag{12}$$

In relation 11, m represents the number of possibilities. According to equation 12, the arrays of the decision matrix can be split by the total of the arrays in the same column to get the matrix P_{ij}. The equation 13 illustrates how to compute P_{ij}. Shannon's entropy connection can be reformulated as equation 13 according to the K equation.

$$E_j = -\frac{1}{\ln(m)} \sum_{i=1}^{m} P_{ij} \ln(P_{ij}) \tag{13}$$

Based on equation 13, the concept of entropy connection for criteria *j* states that the greater the entropy value E_j, the more detrimental its effect on selection. Therefore, equation 14 defines the deviation parameter from entropy for each criterion. The greater the D_j value for each criterion, the more positive its effect on the matrix's weighting.

$$\mathrm{D_j} = 1 - \mathrm{E_j} \tag{14}$$

This weighting is based on the lowest uncertainty value of the *j* criterion (weighting independence from criterion importance), and according to experts, it is unnecessary. The weighted value of each criterion can be computed using equation 15.

$$\mathrm{W_j} = \frac{\mathrm{D_j}}{\sum_{\mathrm{i}=1}^{\mathrm{n}} \mathrm{D_j}} \tag{15}$$

Where, $\mathrm{W_j}$ is the assigned weight value for the *j* criterion. If we want to conduct the combination technique for weighing using Shannon entropy and expert opinion, we can calculate the weighting values for each criterion using equation 16.

$$\acute{\mathrm{W}}_{\mathrm{j}} = \frac{\mathrm{D_j}\lambda_{\mathrm{j}}}{\sum_{\mathrm{i}=1}^{\mathrm{n}} \mathrm{D_j}\lambda_{\mathrm{j}}} \tag{16}$$

In equation 16, λ_{j} represents the effect of the expert's judgment on the weighting of the *j* criterion, whereas $\acute{\mathrm{W}}_{\mathrm{j}}$ represents the total weighting for the *j* criterion. The weighting matrix is in fact a 1×n vector that may be multiplied by the normalized matrix to generate the V matrix. The equation 17 illustrates how to generate the V_{ij} matrix.

$$\mathrm{N} = \begin{bmatrix} n_{11} & \cdots & \mathrm{n_{1*n}} \\ \vdots & \ddots & \vdots \\ \mathrm{n_{m*1}} & \cdots & \mathrm{n_{m*n}} \end{bmatrix}_{\mathrm{m*n}}, W_j = [w_1\ w_2\ w_3 \ldots\ w_n]_{1*n}$$
$$(N_{ij})_{m*n} * (W_j)_{1*n} = V_{ij} \tag{17}$$

Finding positive ideal points (PIS) and negative ideal points (NIS) in the matrix $\mathrm{V_{(m*n)}}$ is accomplished by creating two sets J and G, with the assumption that set J represents the positive impacts and set G represents the negative effects. Thus, the relationship between PIS and NIS is defined as equation18.

$$\begin{aligned} &\mathrm{PIS} = \{\max \mathrm{V_{ij}} | \mathrm{V_{ij}} \in \mathrm{J}\} \text{ or } \{\min \mathrm{V_{ij}} | \mathrm{V_{ij}} \in \mathrm{G}\} \\ &\mathrm{PIS} = [\mathrm{V_1^+}\ \mathrm{V_2^+} \ldots\ldots.. \mathrm{V_n^+}] \\ &\mathrm{NIS} = \{\min \mathrm{V_{ij}} | \mathrm{V_{ij}} \in \mathrm{J}\} \text{ or } \{\max \mathrm{V_{ij}} | \mathrm{V_{ij}} \in \mathrm{G}\} \\ &\mathrm{NIS} = [\mathrm{V_1^-} \mathrm{V_2^-} \ldots\ldots.. \mathrm{V_n^-}] \end{aligned} \tag{18}$$

The Euclidean formula for calculating the distance from the matrices PIS and NIS to the point V_{ij} is equation 19.

$$S_i^+ = \sqrt{\sum_{i=1}^{m} (V_{ij} - V_j^+)^2}$$
$$S_i^- = \sqrt{\sum_{i=1}^{m} (V_{ij} - V_j^-)^2} \tag{19}$$

Each option's relative proximity is defined. Pay close attention to whether the $\mathrm{CL_i}$ parameter is lower or larger in order to make better judgments and decisions. Thus, the greater the value of $\mathrm{CL_i}$ for the *i* option, the more desirable that is option. The expression 20 describes how $\mathrm{CL_i}$ is computed.

$$\mathrm{CL_i} = \frac{\mathrm{S_i^-}}{\mathrm{S_i^+} + \mathrm{S_i^-}} \tag{20}$$

Due to the fixed value of the fraction's denominator, the closer the option is to the intended state, the larger the fraction. The Euclidean distance should therefore be evaluated among the options with the greatest distance. The largest distance from the negative ideal points raises the relative closeness parameter's value for this purpose. The ranking is determined by the $\mathrm{CL_i}$ values. This ranking is performed from greatest to smallest values, meaning that options with a bigger $\mathrm{CL_i}$ are more favorable and those with a smaller $\mathrm{CL_i}$ are less beneficial.

3. RESULTS AND DISCUSSION

Model validation was performed to verify the accuracy of simulation results. This research validates both the independence of the model from the network and the model's consistency with laboratory results. The initial mesh consisted of 26,500 cells with an average size of 22 mm. Combustion pressure readings were used as outputs. By reducing the average grid size of the generated cell values to 45,076,. As the number of cells increased, the combustion pressure output results diverged and deviated from their optimal state. Therefore, the optimally utilized mesh with 45,076 cells was evaluated. Figure 3 demonstrates how to validate and test the mesh's independence.

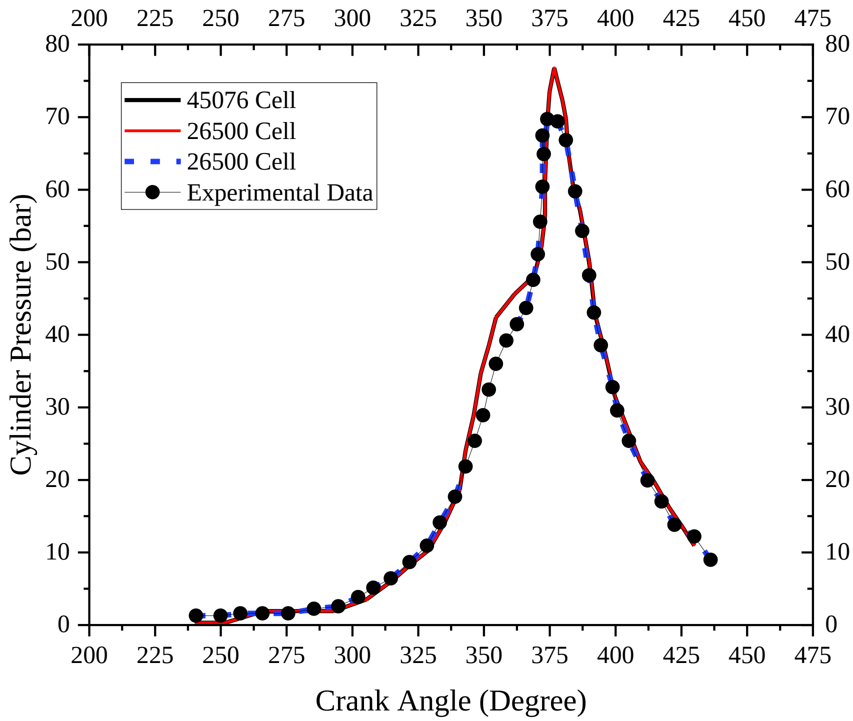

Figure 3. Validation and test of grid independence.

A comparison was done between the laboratory data and the computer model to assess the difference between the numerical study and other researchers' experimental investigations. Upon comparing the simulation and laboratory data, it was found that there is an error margin of approximately 10% between the simulation and experimental results. Consequently, the outputs of the simulation model are consistent with the findings from the laboratory. Figure 4 illustrates the validation of simulation results with laboratory data.

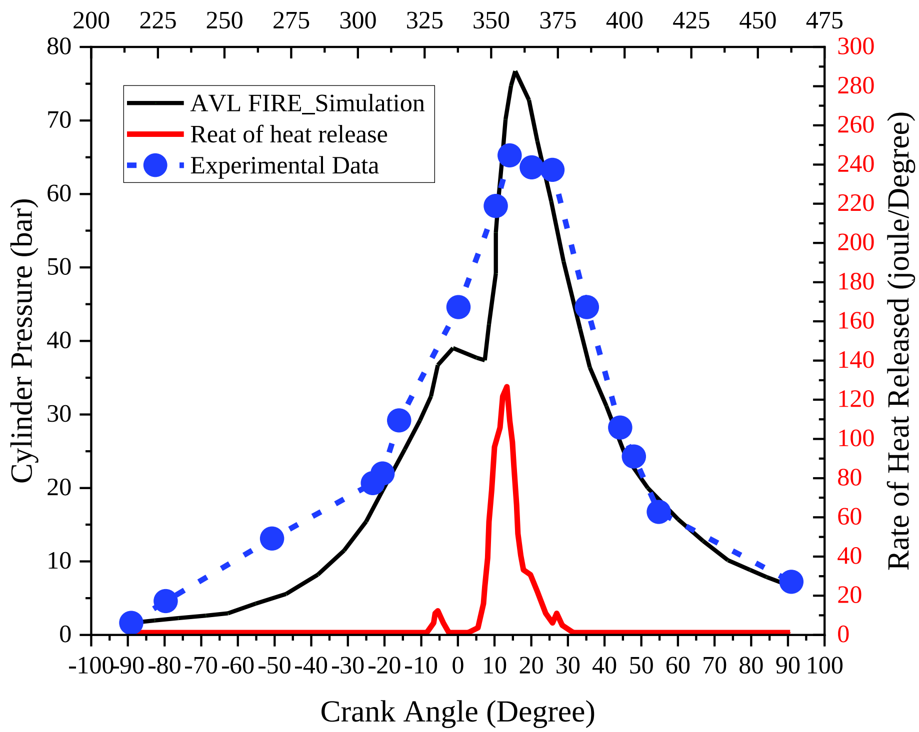

Figure 4. Validation of simulation results with laboratory results.

3.1. Optimization Modeling Using RSM Method

CO and NOx emissions can be modeled using a square model. The estimation error of the output is 0.2435 when using the square model. In addition, a value of 0.3974 was recorded for the square method estimation of the modeling error for NOx production. At a significance level of 5%, neither the independent variables nor the interaction effects between them may significantly impact the changes in engine emissions. However, if a significance threshold of 10% is considered, the results of the ANOVA analysis may change. The emissions of CO pollutants are greatly influenced by two variables: the starting time of fuel injection and the interaction between compression ratio and injection angle. This was determined through an ANOVA analysis with a significance level of 0.10. In the study of oxides, nitrogen has a significant impact on both the start time of spraying (an independent variable) and the output variable, which is affected by the square of the spraying angle. However, the analysis of the input factors indicates that variations in the compression ratio and injection angle parameters have minimal influence on the significant level of emissions generated by the engine under investigation. By analyzing the lack of fit parameters, it can be concluded that the NOx pollutant emission model is not significantly influenced by the selected parameters or their interactions (with a significance level of 0.1). Three-dimensional graphs of the response surface can be used to explore the mutual effects of variables on changes in pollution emissions. The smallest amount of CO pollutant emissions is achieved by using the shortest starting injection time and compression ratio, as these two factors interact with each other. In other words, carbon monoxide emissions are positively correlated with the input parameters of compression ratio and spraying start time. The same effect is observed between the variables of injection angle and fuel injection start time. Delaying the timing of the spray allows for the possibility of reducing both the compression ratio and spray angle, thereby minimizing the emission of CO. However, the combined impact of compression ratio and spray angle on CO pollutant emission is not always conducive to minimizing it. Therefore, to achieve the lowest possible CO emission, it is necessary to find a balance between reducing the compression ratio and adjusting the spray angle. Figures 5 and 6 each illustrate three interactions for their respective results.

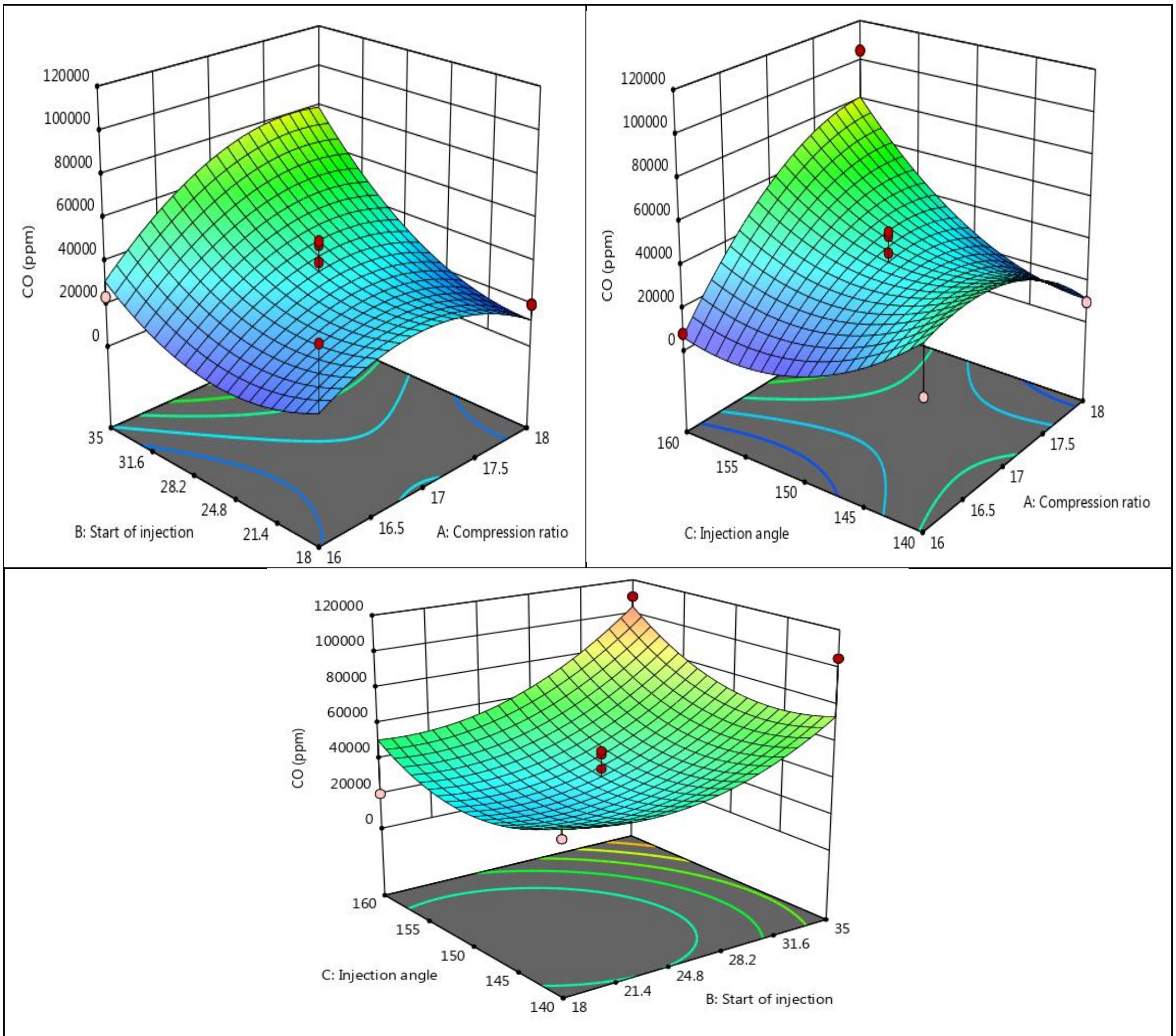

Figure 5. analyzing the interplay between input factors and CO emissions.

In order to limit NOx emissions by adjusting input parameters, the compression ratio should be considered in conjunction with the injection start delay. Contrary to the goal of minimizing CO emissions, there is an inverse correlation between NOx emissions and compression ratio and injection start time. Analyses of two parameters, the spraying angle and the start time of spraying, reveal the same impact. The correlation between the injection angle and compression ratio in reducing NOx and CO emissions remains consistent throughout the observed trend of changes.

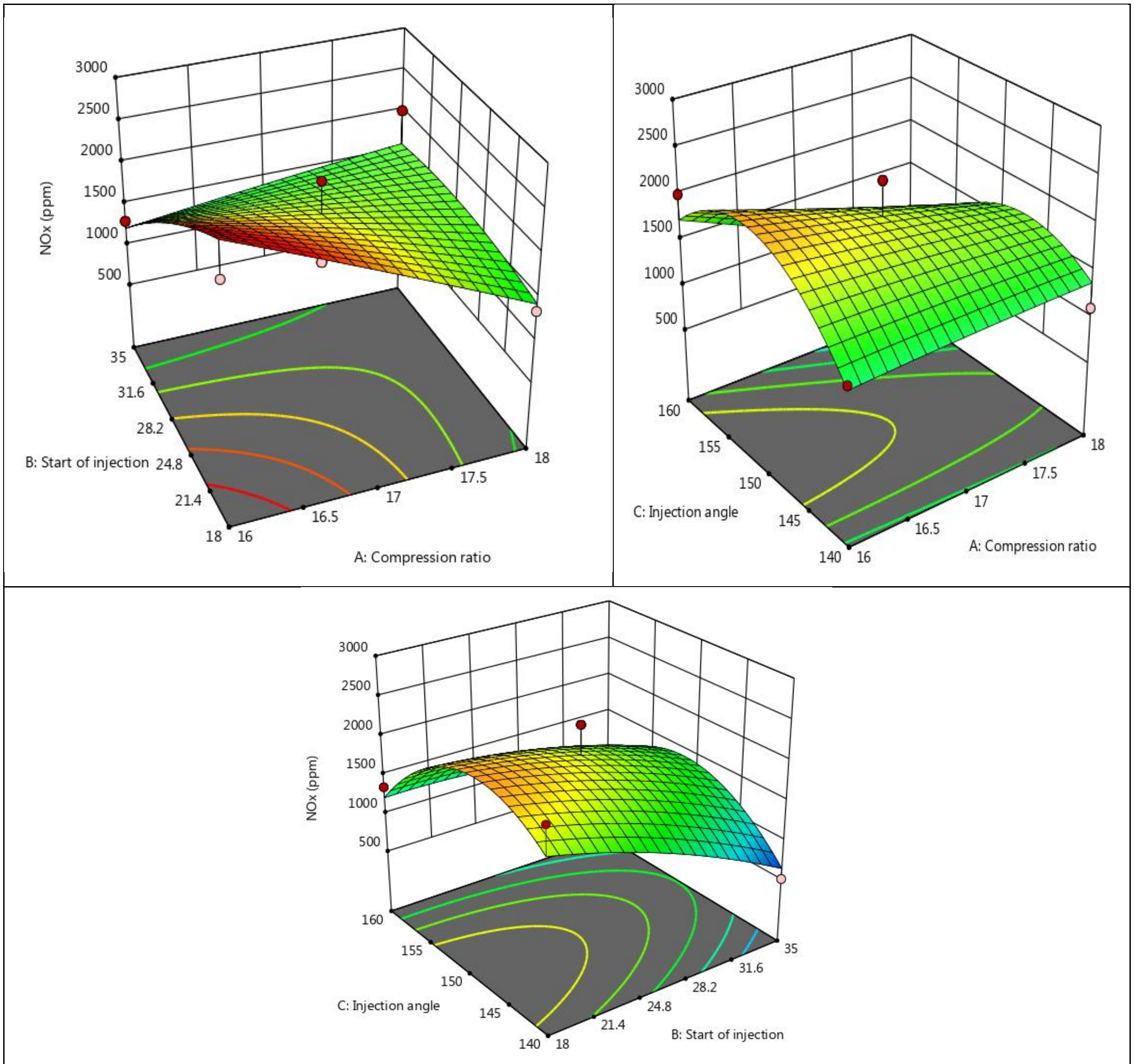

Figure 6. Studying the interaction effect of input variables on NOx emission.

Optimizing the impact of CO and NOx pollutants, as demonstrated by the response surface method, suggests that further investigation into the advancement of injection timing is necessary, and the range of its variation should be expanded. The highest level of CO and NOx output reduction was achieved at 81.6% availability.

3.2. Optimization Modeling Using Taguchi Method

Utilizing regression analysis and assessing the accuracy of modeling were considered the most crucial parameters in Taguchi analysis. This study aimed to optimize the Taguchi technique using the "bigger is better" objective. The signal-to-noise ratio (S/N) of the majority of input components is not statistically significant ($P<0.05$). This condition indicates that all factors and their chosen levels have a direct effect on the changes in response levels of the output variables. None of the factors and their chosen levels should be considered as test noise. The Delta index was used to analyze the impact of each parameter on the output variable's response. The start time of fuel injection and the percentage of CNG fuel mixing have the biggest impact on determining the reaction, compared to the noise signal of the outputs. Taguchi's approach aims to optimize S/N effect of each variable. In this context, as the fuel percentage increases, the CNG fuel component also grows, and so does the S/N response. This positive trend indicates that increasing the CNG fuel percentage is beneficial. The composition of the fuel has a greater impact on the output parameters. However, as the amount of fuel increases, it deviates from the optimal condition's average, causing the output variables to become more scattered and less correlated. Variations in other parameters have not been uniform. The start time for spraying has a significant impact on output parameters. When spraying is initiated earlier, there is an upward trend in output parameters. However, this trend deviates significantly from the mean values between 20 to 30 degrees before the top dead point. It has been explained that increasing the compression ratio within the range of 16 to 17 can effectively improve engine output indicators while maintaining normal limits for response of output variables. Additionally, the influence of the spray angle parameter and compression ratio decreases. Figure 7 depicts the S/N diagram.

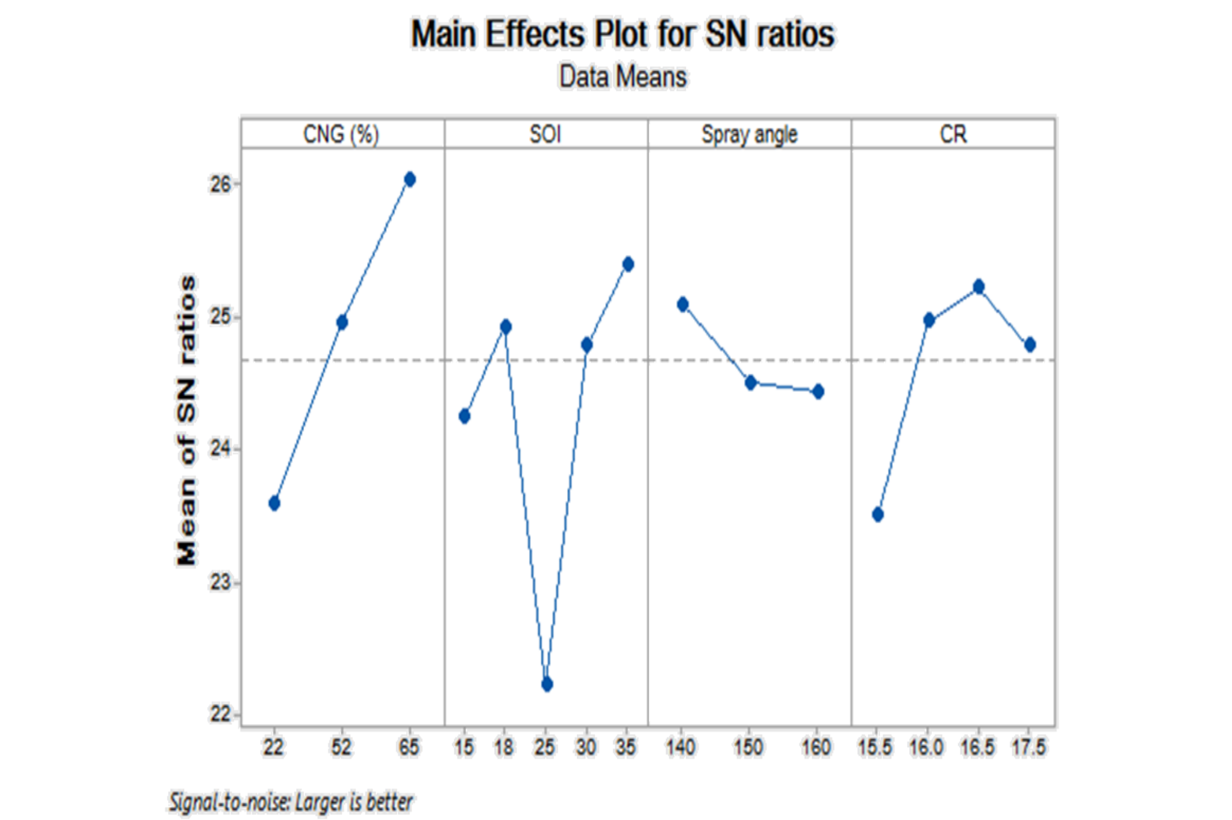

Figure 7. The S/N ratio and fit and correlation diagrams of output variables.

Similar to examining the noise effect of factors, analyzing the influence of averages demonstrates the direct impact of CNG fuel on improving performance indicators and reducing emissions. With the exception that raising the fuel mixture percentage has a detrimental impact on the improvement of performance indicators and engine emissions. During the examination of the fuel injection angle index, it was observed that the reverse trend of increasing the injection angle between 140 and 150 did not result in any significant changes. Both of these values were found to be close to the mean. However, a 10-degree increase relative to the 150-degree mark has diminished the favorable effects of the output variables. In addition, increasing the compression ratio has improved the engine's performance and emissions. However, increasing it from 16.5 to 17.5 has resulted in a significant decrease in engine performance and emissions. Through an analysis of the Delta factor, it was determined that the percentage of fuel mixture and the timing of injection had the greatest impact on the variations in the average reaction rate of the outputs. Therefore, when estimating the output variables based on the mean value, it is important to first examine the percentage of fuel mixture and then the fuel injection start time.

3.3. Optimization Modeling Using Multi-Criteria Decision Making

After reviewing and studying the TOPSIS selection technique, we have concluded that the third decision yields the lowest fuel consumption and highest thermal efficiency, while the twentieth decision results in the opposite. Therefore, increasing the compression ratio, advancing the injection start time, and optimizing the injection angle can effectively reduce fuel consumption and maximize the thermal efficiency of the dual-fuel diesel/gas engine during braking. By emphasizing this approach, the ninth option could also function as a substitute for the optimal solution. Figure 8a illustrates how the parameter for relative proximity distance (CL) varies for each decision. By analyzing the optimal selection technique, we have determined that reducing the proportion of gas fuel actually increases fuel consumption. As a result of the decrease in the share of natural gas fuel, more air enters the combustion chamber. The oxygen sensor then signals the electronic control system to increase the amount of basic fuel injection, which leads to an increase in fuel consumption. In the functional method, the optimal decision is the one that generates the highest output values for the functional parameters. Upon examining the changes in the relative proximity distance variable for the variables that define the engine's functional approach, it becomes evident that the third decision's relative proximity parameter represents the most optimal option. Additionally, the 20th option will be the farthest option. The consistency in modifying parameters demonstrates the close relationship between the functional and economic approaches. If the engine user wants to make a decision that simultaneously minimizes fuel consumption and maximizes engine performance, they can utilize economic by adjusting the engine input parameters in the third mode of decision-making. User-friendly functionality is an important consideration in both economic and functional approaches. When analyzing the relative closeness distance parameter graphically, a significant difference is observed. The optimal choice decreases sharply as the percentage of natural gas fuel in the combustion chamber decreases. Reducing the percentage of natural gas fuel and increasing the percentage of injected fuel can lead to inhomogeneous combustion conditions, which can decrease performance metrics. It should be emphasized that the three parameters influencing the economic approach's judgments are directly related to the engine's performance characteristics. The comparability of the modifications made to the selection parameter of the relative proximity distance in the two methods is justifiable. Figure 8b illustrates how the parameter for relative CL changes for each decision.

As with the previous two techniques, the optimal decision in environmental strategy is the one that produces the least amount of pollution emissions and exhaust gas heat. The research on response surface method revealed that the modeling of CO and NOx emissions exhibited a nearly monotonic behavior. Due to the simple structure of hydrocarbon molecules in the fuel mixture of the diesel/gas dual fuel engine, an increase in both NOx emissions and exhaust gas temperature can be expected. However, modeling results have revealed that there is also an increase in CO in engines of this type. Therefore, there is a distinction between the optimal choice and alternative approaches when selecting the best environmental decision. Based on the analysis of the relative closeness distance parameter, the 18th option is the optimal alternative for minimizing emissions and exhaust gas. The sixteenth decision represents the greatest deviation from the intended location. The difference between these two decisions lies in the changes to the compression ratio. Increasing the compression ratio creates more space to receive the fuel mixture and also increases the maximum capacity of the combustion pressure. However, this also simultaneously increases emissions and the temperature of the engine's exhaust gases. To implement an environmentally-friendly approach in the engine being examined, the optimal method is to focus on managing the fuel mixture percentage and advancing the fuel injection start time. Figure 8c illustrates how the parameter for relative CL varies for each decision.

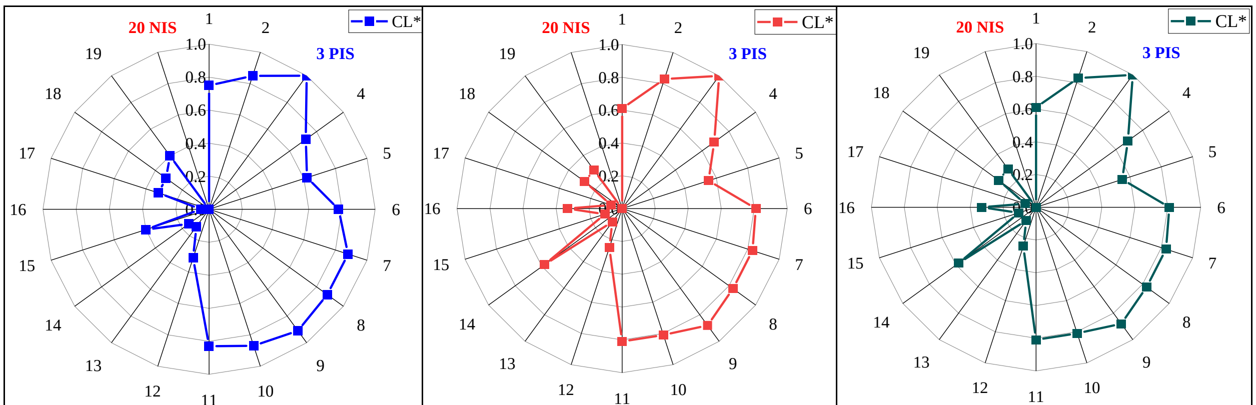

a b c

Figure 8. How the relative CL parameter varies with each economic approach decision.

$\mathrm{PIS}_a = \mathrm{CNG} = 52, \mathrm{SOI} = 15, \mathrm{SA} = 160, \mathrm{CR} = 17.5$ $\mathrm{NIS}_a = \mathrm{CNG} = 22, \mathrm{SOI} = 35, \mathrm{SA} = 140, \mathrm{CR} = 16$

$\mathrm{PIS}_b = \mathrm{CNG} = 52, \mathrm{SOI} = 15, \mathrm{SA} = 160, \mathrm{CR} = 17.5$ $\mathrm{NIS}_b = \mathrm{CNG} = 22, \mathrm{SOI} = 35, \mathrm{SA} = 140, \mathrm{CR} = 16$

$\mathrm{PIS}_c = \mathrm{CNG} = 22, \mathrm{SOI} = 30, \mathrm{SA} = 160, \mathrm{CR} = 16$ $\mathrm{NIS}_c = \mathrm{CNG} = 22, \mathrm{SOI} = 30, \mathrm{SA} = 160, \mathrm{CR} = 17.5$

4. Results and Discussion

This study utilized two modeling methods and a multi-criteria decision-making approach to evaluate the performance parameters and emissions of a dual-fuel diesel/gas engine. The response surface method was used to model three variables, injection angle, injection start time, and compression ratio, to study pollution emissions. During the experimental planning phase, it was discovered through modeling and ANOVA analysis that the two factors of spraying start time and the interaction between compression ratio and spraying angle had a significant impact on changes in CO pollutants ($P < 0.1$). The modeling error for CO emissions is 25%, and for nitrogen oxide emissions, it is 39%. During the response surface modeling, it was discovered that the outputs did not correspond to nitrogen oxide emissions, suggesting the involvement of another factor in the modeling of such emissions. Additionally, a significant impact on nitrogen oxide emissions was observed due to the fuel injection timing, and the square of the injection angle. The impact of independent factors on the modeling of CO and nitrogen oxide emissions is unclear, and optimization is necessary to reduce pollutant emissions. Considering the relative importance of emissions of nitrogen oxides and carbon monoxide in dual-fuel diesel/gas engines, a single-objective optimization was performed. It was possible to achieve 81.6% of the objective function for minimizing emissions. Furthermore, the optimization results indicate that in order to minimize the discharge of pollutants, the range of change for two independent variables, namely density ratio and spraying start time, should be expanded. Taguchi modeling results demonstrate that the natural gas fuel percentage parameter has a significant effect on the modeling of emission and performance parameters. Due to the non-orthogonality of the independent variables, which is caused by the lack of uniform stratification, the response level method method is more accurate than modeling based on the average effect and noise effect (S/N). In order to implement multi-criteria decision-making, the output parameters were categorized into three approaches: economic, functional, and environmental. Specific braking fuel consumption, indicative specific fuel consumption, and braking thermal efficiency are factors that influence the economic approach. Torque, indicative power, average effective braking pressure, and indicator are parameters that influence the functional approach. Emissions of CO and NOx, as well as gas heat, are factors that influence the environmental approach. The engine's output was considered one of the parameters that impacted the environmental approach. Due to the interdependence of the economic approach's parameters on the functional approach's parameters, the relative closeness index (CL) yielded identical results in both approaches. The optimal approach for reducing fuel consumption, boosting efficiency, and enhancing performance parameters is to increase the compression ratio and injection angle, use 50% natural gas fuel, and decrease injection time. In contrast to the functional and economic approaches, the environmental approach showed little sensitivity to changes in the density ratio. Increasing the spraying angle and adjusting the spraying start time reduced the number of parameters that affect the environmental impact. Reducing the percentage of natural gas fuel also brought the outputs closer to the ideal operating state.

5. References

[1] M. Esmaeili Shayan, G. Najafi, G. Lorenzini, Phase change material mixed with chloride salt graphite foam infiltration for latent heat storage applications at higher temperatures and pressures, Int. J. Energy Environ. Eng. 2022 (2021) 1–11. https://doi.org/10.1007/s40095-021-00462-5.

[2] M. Gülüm, Effects of compression ratio, blending ratio and engine speed on fuel cost, performance and exhaust emissions of a diesel engine fueled with bio-derived alternative fuels, Sustain. Energy Technol. Assessments. 53 (2022) 102464. https://doi.org/10.1016/J.SETA.2022.102464.

[3] M. Esmaeili Shayan, G. Najafi, B. Ghobadian, S. Gorjian, M. Mazlan, A novel approach of

synchronization of the sustainable grid with an intelligent local hybrid renewable energy control, Int. J. Energy Environ. Eng. 2022. (2022) 1–12. https://doi.org/10.1007/S40095-022-00503-7.

[4] Y. Hua, Z. Wang, R. Li, S. Liu, Y. Zhao, L. Qu, D. Mei, H. Lv, Experimental study on morphology, nanostructure and oxidation reactivity of particles in diesel engine with exhaust gas recirculation (EGR) burned with different alternative fuels, Energy. 261 (2022) 125249. https://doi.org/10.1016/J.ENERGY.2022.125249.

[5] W. Zhao, J. Yan, S. Gao, T.H. Lee, X. Li, The combustion and emission characteristics of a common-rail diesel engine fueled with diesel and higher alcohols blends with a high blend ratio, Energy. 261 (2022) 124972. https://doi.org/10.1016/J.ENERGY.2022.124972.

[6] M.M. Abdelaal, A.H. Hegab, Combustion and emission characteristics of a natural gas-fueled diesel engine with EGR, Energy Convers. Manag. 64 (2012) 301–312. https://doi.org/10.1016/J.ENCONMAN.2012.05.021.

[7] J. Liu, F. Yang, H. Wang, M. Ouyang, S. Hao, Effects of pilot fuel quantity on the emissions characteristics of a CNG/diesel dual fuel engine with optimized pilot injection timing, Appl. Energy. 110 (2013) 201–206. https://doi.org/10.1016/J.APENERGY.2013.03.024.

[8] Z. Liu, G.A. Karim, A Predictive Model for the Combustion Process in Dual Fuel Engines, SAE Tech. Pap. (1995). https://doi.org/10.4271/952435.

[9] L. De Simio, S. Iannaccone, Gaseous and particle emissions in low-temperature combustion diesel–HCNG dual-fuel operation with double pilot injection, Appl. Energy. 253 (2019) 113602. https://doi.org/10.1016/J.APENERGY.2019.113602.

[10] T. Tsujimura, Y. Suzuki, The utilization of hydrogen in hydrogen/diesel dual fuel engine, Int. J. Hydrogen Energy. 42 (2017) 14019–14029. https://doi.org/10.1016/J.IJHYDENE.2017.01.152.

[11] T. Anandavelu, S. Rajkumar, V. Thangarasu, Dual fuel combustion of 1-hexanol with diesel and biodiesel fuels in a diesel engine: An experimental investigation and multi criteria optimization using artificial neural network and TOPSIS algorithm, Fuel. 338 (2023) 127318. https://doi.org/10.1016/J.FUEL.2022.127318.

[12] A. Tarafdar, P. Majumder, M. Deb, U.K. Bera, Performance-emission optimization in a single cylinder CI-engine with diesel hydrogen dual fuel: A spherical fuzzy MARCOS MCGDM based Type-3 fuzzy logic approach, Int. J. Hydrogen Energy. (2023). https://doi.org/10.1016/J.IJHYDENE.2023.04.019.

[13] M. Mahdi Teymoori, I. Chitsaz, A. Zarei, Three-way catalyst modeling and fuel switch optimization of a natural gas bi-fuel-powered vehicle, Fuel. 341 (2023) 126979. https://doi.org/10.1016/J.FUEL.2022.126979.

[14] X. Ping, B. Yao, H. Zhang, F. Yang, Thermodynamic, economic, and environmental analysis and multi-objective optimization of a dual loop organic Rankine cycle for CNG engine waste heat recovery, Appl. Therm. Eng. 193 (2021) 116980. https://doi.org/10.1016/J.APPLTHERMALENG.2021.116980.

[15] J. Jung, S. Song, K.B. Hur, Numerical study on the effects of intake valve timing on performance of a natural gas-diesel dual-fuel engine and multi-objective Pareto optimization, Appl. Therm. Eng. 121 (2017) 604–616. https://doi.org/10.1016/J.APPLTHERMALENG.2017.03.036.

[16] T. Zhou, J. Liu, J. Liu, J. Ren, S. Ding, S. Yang, Energy-exergy-economic-environmental (4E) analysis and multi-objective optimization of a cascade LiBr/H2O refrigeration and Organic Rankine cycle integrated system for power generation, Appl. Therm. Eng. 225 (2023) 120142. https://doi.org/10.1016/J.APPLTHERMALENG.2023.120142.

[17] P. Jena, R. Raj, J.V. Tirkey, Thermodynamic performance study and RSM based optimization of SI engine using sewage sludge producer gas blend with methane, Energy. 273 (2023).

https://doi.org/10.1016/j.energy.2023.127179.

[18] M.F. Al-Dawody, W. Al-Obaidi, E.D. Aboud, M.A. Abdulwahid, K. Al-Farhany, W. Jamshed, M.R. Eid, Z. Raizah, A. Iqbal, Mechanical engineering advantages of a dual fuel diesel engine powered by diesel and aqueous ammonia blends, Fuel. 346 (2023) 128398. https://doi.org/10.1016/J.FUEL.2023.128398.

[19] H.E. Gulcan, M. Ciniviz, Experimental study on the effect of piston bowl geometry on the combustion performance and pollutant emissions of methane-diesel common rail dual-fuel engine, Fuel. 345 (2023) 128175. https://doi.org/10.1016/J.FUEL.2023.128175.

[20] H. Tarigonda, B. Anjaneyulu, R. Raghurami Reddy, K.L. Narasimhamu, Optimization of performance and emission characteristics of a diesel engine in dual-fuel mode with LPG using adaptive-neuro fuzzy inference system model, Mater. Today Proc. (2023). https://doi.org/10.1016/J.MATPR.2023.02.290.

[21] D. Goyal, T. Goyal, S.K. Mahla, G. Goga, A. Dhir, D. Balasubramanian, A.T. Hoang, M. Wae-Hayee, J.S.F. Josephin, A. Sonthalia, E.G. Varuvel, K. Brindhadevi, Application of Taguchi design in optimization of performance and emissions characteristics of n-butanol/diesel/biogas under dual fuel mode, Fuel. 338 (2023) 127246. https://doi.org/10.1016/J.FUEL.2022.127246.

[22] L. Xiang, G. Theotokatos, Y. Ding, Parametric investigation on the performance-emissions trade-off and knocking occurrence of dual fuel engines using CFD, Fuel. 340 (2023). https://doi.org/10.1016/j.fuel.2023.127535.

[23] L. Zhu, B. Li, A. Li, W. Ji, Y. Qian, X. Lu, Z. Huang, Effects of fuel reforming on large-bore low-speed two-stroke dual fuel marine engine combined with EGR and injection strategy, Int. J. Hydrogen Energy. 45 (2020). https://doi.org/10.1016/j.ijhydene.2020.07.266.

[24] B. Yang, L. Ning, B. Liu, G. Huang, Y. Cui, K. Zeng, Comparison study the particulate matter characteristics in a diesel/natural gas dual-fuel engine under different natural gas-air mixing operation conditions, Fuel. 288 (2021). https://doi.org/10.1016/j.fuel.2020.119721.

[25] H. Hazar, T. Telceken, H. Sevinc, An experimental study on emission of a diesel engine fuelled with SME (safflower methyl ester) and diesel fuel, Energy. 241 (2022) 122915. https://doi.org/10.1016/J.ENERGY.2021.122915.

[26] D. Kumar, U. Sonawane, K. Chandra, A.K. Agarwal, Experimental investigations of methanol fumigation via port fuel injection in preheated intake air in a single cylinder dual-fuel diesel engine, Fuel. 324 (2022) 124340. https://doi.org/10.1016/J.FUEL.2022.124340.

[27] V.N. Adrian, N.D. Catalin, C. Radu, On some possible effects of using renewable oxygenated fuels in a large marine diesel engine, Energy Reports. 8 (2022) 966–977. https://doi.org/10.1016/J.EGYR.2022.07.129.

[28] X. Sun, M. Xie, F. Zhou, J. Fu, J. Liu, Multi-objective optimization for combustion, thermodynamic and emission characteristics of Atkinson cycle engine using tree-based machine learning and the NSGA II algorithm, Fuel. 342 (2023). https://doi.org/10.1016/j.fuel.2023.127839.

[29] Z. Said, D.T.N. Le, P. Sharma, V.H. Dang, H.S. Le, D.T. Nguyen, T.A.E. Bui, V.G. Nguyen, Optimization of combustion, performance, and emission characteristics of a dual-fuel diesel engine powered with microalgae-based biodiesel/diesel blends and oxyhydrogen, Fuel. 326 (2022) 124987. https://doi.org/10.1016/J.FUEL.2022.124987.

[30] D. Tan, Y. Wu, J. Lv, J. Li, X. Ou, Y. Meng, G. Lan, Y. Chen, Z. Zhang, Performance optimization of a diesel engine fueled with hydrogen/biodiesel with water addition based on the response surface methodology, Energy. (2022) 125869. https://doi.org/10.1016/J.ENERGY.2022.125869.

[31] Z. Said, P. Sharma, B.J. Bora, V.N. Nguyen, T.A.E. Bui, D.T. Nguyen, X.T. Dinh, X.P. Nguyen,

Modeling-optimization of performance and emission characteristics of dual-fuel engine powered with pilot diesel and agricultural-food waste-derived biogas, Int. J. Hydrogen Energy. (2022). https://doi.org/10.1016/J.IJHYDENE.2022.07.150.

[32] A.K. Agarwal, Prashumn, H. Valera, N. Nath Mustafi, Di-ethyl ether-diesel blends fuelled off-road tractor engine: Part-II: Unregulated and particulate emission characteristics, Fuel. 308 (2022) 121973. https://doi.org/10.1016/J.FUEL.2021.121973.

[33] A. Kolakoti, H. Koten, Effect of supercharging in neat biodiesel fuelled naturally aspirated diesel engine combustion, vibration and emission analysis, Energy. 260 (2022) 125054. https://doi.org/10.1016/J.ENERGY.2022.125054.

[34] A. Tuan Hoang, M. Xuan Le, S. Nižetić, Z. Huang, Ü. Ağbulut, I. Veza, Z. Said, A. Tuan Le, V. Dung Tran, X. Phuong Nguyen, Understanding behaviors of compression ignition engine running on metal nanoparticle additives-included fuels: A control comparison between biodiesel and diesel fuel, Fuel. 326 (2022) 124981. https://doi.org/10.1016/J.FUEL.2022.124981.

[35] C. Fei, Z. Qian, Z. Yang, J. Ren, S. Zhu, Y. Yan, Z. Shu, Combustion and emission performance of isopropanol-butanol-ethanol (IBE) mixed with diesel fuel on marine diesel engine with nano YSZ thermal barrier coating, Energy. 256 (2022) 124683. https://doi.org/10.1016/J.ENERGY.2022.124683.

[36] S.P. Ramachandran, A. Shrivastava, A. Sharma, M. Feroskhan, R. Manoj Kuma, S.M. Dasharath, Performance, emission and combustion characteristics of a biogas–diesel dual fuel engine using Taguchi method, Mater. Today Proc. 54 (2022) 548–556. https://doi.org/10.1016/J.MATPR.2022.02.194.

[37] R. Rohith Renish, G. Maneesha, P. Jeyaraman, T. Niruban Projoth, Experimental investigation on performance and emissions of a VCR engine fuelled by biodiesel/diesel blends, Mater. Today Proc. 62 (2022) 3689–3698. https://doi.org/10.1016/J.MATPR.2022.04.427.

[38] D. Kumar Singh, R. Raj, J.V. Tirkey, Performance and emission analysis of triple fuelled CI engine utilizing producer gas, biodiesel and diesel: An optimization study using response surface methodology, Therm. Sci. Eng. Prog. (2022) 101486. https://doi.org/10.1016/J.TSEP.2022.101486.